EUROPEAN LABORATORY FOR PARTICLE PHYSICS

LHCb 2000–42
CALO
25 June 2000

Design and Construction of the LHCb Scintillator Pad/Preshower Detector

S. Filippov, Yu. Gavrilov, E. Guschin[a)], V. Klubov, L. Kravchuk, S. Laptev, V. Postoev, A. Sadovsky

Institute for Nuclear Research
Russian Academy of Sciences
60th October Anniversary Prospekt 7A
RU–117312 Moscow

LHCb Collaboration

Abstract

General approach to design and construction of LHCb SPD/PS detector is described.

[a)] Corresponding author, E-mail: Evgueni.Gouchtchine@cern.ch

1 Introduction

Preshower (PS) detector and Scintillator Pad Detector (SPD) are proposed to be implemented in the LHCb-b experiment [1] for better electron/photon identification and hadron discrimination at the level-0 trigger. Preshower information used together with information from ECAL and HCAL provides electron/pion separation at the stage of off-line data analysis. SPD/PS detector uses scintillator pad readout by wavelength-shifting (WLS) fibres coupled to multi-anode photo-multiplier tubes (MaPMT) via clear plastic fibres. This technique is commonly used during last years in many experiments [2, 3, 4]. The specific features of SPD/PS detector are rather high granularity in the inner part and usage of PMT with small ($2 \times 2\ mm^2$) pixels. It enables to create a fast, multichannel pad detector with low cost per channel.

In this paper we describe general design, detector elements and mechanical support, including detector construction and assembly scheme.

The content of the note is subdivided by sections as follows:

- General layout and geometry of SPD/PS are described in Sec. 2.
- Mechanical Support is in Sec. 3
- Description and construction of scintillator cell can be found in Sec. 4.
- Description of detector unit design and assembly is in Sec. 5
- Design and assembly of supermodule is in Sec. 6
- Description of assembly of whole detector is in Sec. 7
- Monitoring system idea is described in Sec. 8
- Quality control is in Sec. 9

2 General layout and geometry of SPD/PS detector

The SPD/PS detector planes are to be installed into the space between the first muon chamber M1 and ECAL. The layout of the SPD/PS detector is shown in Fig. 1-3. It consists essentially of two identical rectangular scintillator planes of high granularity with 11904 detection channels of **scintillator pads**. The sensitive area of the detector is 7.6 m in width and 6.2 m in hight. Due to projectivity from IP all dimensions of the SPD plane are smaller than those of the PS one by $\sim 0.45\%$. The detector planes are divided into two halves, each of them can slide independently on horizontal rails to the left and right sides of a frame for the service and maintenance works. In between the SPD and PS detector planes there is an immovable lead converter of $\sim$2 X0 thickness (12 mm). The distance along beam axis between centres of PS and

SPD scintillator planes is 56 mm. The arrangement of cells is one to one projective correspondence with ECAL towers. Therefore each PS and SPD plane is subdivided into inner, middle and outer parts with $\sim 4 \times 4$, 6×6 and 12×12 cm^2 cell sizes (see Table 1). Pad size is a net dimension of scintillator that differs from the cell size by thickness of scintillator pad wrapping and detector unit walls, see Fig. 4.

Table 1: Basic geometrical parameters of SPD/PS planes.

Region	Dimensions of SPD (cm)	Dimensions of PS (cm)	SPD cell size (mm)	PS cell size (mm)	Number of cells (PS+SPD)
Inner	190.5 x 143	191.4x 143.5	39.66	39.84	1472 x 2 = 2944
Middle	381 x 238	382.7 x 239	59.5	59.76	1792 x 2 = 3584
Outer	762 x 619	765.5 x 622	119	119.5	2688 x 2 = 5376

The cells are packed in $\sim 48 \times 48$ cm^2 boxes (**detector units**) that are joined into **supermodules**. Each supermodule has ~ 96 cm width and ~ 6.5 m hight and consists of 13 rows by 2 columns of detector units.

The scintillator thickness is 15 mm. According to beam test measurements [5] it is enough to have a statistics of 30 photoelectrons for MIPs. The total weight of plastic scintillator to be mounted on the SPD/PS planes is ~ 1500 kg. The total area to be covered by scintillator cells for both SPD/PS planes is ~ 94 m^2.

A square hole of 48×48 cm^2 will be introduced in the central part of the detector to accommodate the beam pipe. The total weight of immovable 12 mm thick lead converter fixed in between the PS and SPD planes is about $8,200$ kg. In comparison, the weight of the movable one half of the detector plane is $\sim 1,600$ kg (see Table 2).

The space reserved for SPD/PS detector between the first muon chamber and ECAL is 180 mm only. This makes its conceptual and technical design rather complicated.

The detailed geometry of the detector along the beam axis is shown in Fig. 5. The material budget for Monte-Carlo simulation can be taken from this drawing. In order to minimise the γ conversions in the aluminium support of SPD supermodules it can be replaced by a grid structure or aluminium profile with the reduction of the amount of aluminium up to at least 3 times. If necessary, the covers of the SPD modules can be made of plastic. For the assembly of the boxes aluminium screws can be used. All this allows to reduce probability of γ conversion before the SPD scintillator layer from 7% to $1 - 2\%$. To make a final choice of the design, one has also to account all the material budget from IP to SPD.

Table 2: Main parameters of mechanical structure.

Structure	Material	Z-X Cross-section	Y-Length	Weight,kg
Detector + Support				**19,570**
Main Support Beams	Steel	200 cm^2	19 m	2,900
Base Beam	Steel	90 cm^2	19 m	1,300
Lead wall	Lead	12 $mm \times 7.9$ m	7.7 m	8,200
$4 \times 1/2$ detector		2×7 $cm \times 7.7$ m	7.6 m	6,320
lower support beam	Steel	124 cm^2	9 m	850
1/2 Detector		7 $cm \times 7.7$ m	3.8 m	**1,580**
Carriage	Steel	24 cm^2	4.5 m	80
4 supermodules		7 $cm \times 7.7$ m	4×96 cm	4×374
Supermodule		7 $cm \times 7.7$ m	96 cm	**374**
Support Strip	Al	6 $mm \times 6.7$ m	96 cm	106
PMTs Support Plates	Steel	225 cm^2	96 cm	164
2×13 detector units				26×4
Whole Scintillator	Sci	2×15 $mm \times 6.2$ m	7.6 m	**1,500**

3 Mechanical support

The general scheme of mechanical support is shown Figs. 1-3. The basic element of the SPD/PS detector support is the main beam that is fixed to the gantries running on both sides above LHCb detector. The main beam is rigid enough to hold all mechanical support structure and SPD/PS detector with total weight about 20 t without significant deflection under load.

The main element of the SPD/PS detector providing precise geometrical position is a base beam hanged up by a set of adjustable screws to the main beam. It holds both lead converter and SPD/PS detector. Tuning the set of adjustable screws it is possible to correct deformation of the basic beam arising under load of lead and detector over all it's length. One can smooth the bend of the basic beam and correct position of the detector as well as converter in a vertical plane.

Each half of SPD/PS detector consisting of four supermodules is hanged up on a separate carriage moving along one of the two rails on the basic beam. The supermodules are fixed by screws. Tuning them the precise vertical position of each supermodule can be done. The adjoining supermodules are attached to each other with a flat hinges. Thus each detector' half can be independently moved out of the working position for assembly or service works.

The lead converter once installed at the place is immovable. The bottom edges of the detector are freely inserted in guide-ways mounted on the lower supporting beam, to which the bottom of lead wall is fixed too. This allows the side movement and fixing the Z-position of the detector.

Main physical parameters of mechanical structure and detector elements are shown in Table. 2. Further optimisation of support structure could reduce the total weight, mainly of the main beam, by $\sim 1\ t$.

4 The scintillator cells and the WLS fibre system

The granularity of the SPD/PS detector is determined by the tower sizes of ECAL towers in accordance with projectivity from IP. Therefore the SPD/PS scintillator planes are separated into three regions: inner, middle and outer, each having a different pad size (Fig. 4).

4.1 Pad design and construction

Fig. 4 shows the geometry of an individual scintillator pad with WLS fibre layout. The scintillator pads will be produced from the plastic manufactured in Russia. The basic plastic component is polystyrene to which primary and secondary wave-length shifting dopants (PTP, 1.5% and POPOP, 0.04%) are added. We have chosen 1.0 mm diameter Y11(250) multi-cladding S-type WLS fibre from KURARAY [6] as a reasonable compromise between light output and durability. The S-type is more resistant to bending and cracking [7], that is very important for readout design, especially for the smallest pads in the inner region. Light produced by an ionising particle inside the scintillator is absorbed by WLS fibre, and re-emitted green light is guided by total internal reflection to the PMT.

A square structure of the pads will be cut out from a 15 mm thick scintillator plate, and all scintillator surface will be polished with an optical quality. To increase the light collection the coils of WLS fibre are placed into the ring groove milled in the body of the cell using the CNC machine. The cross section of the groove has a rectangular form with a 4.1 mm depth and 1.1 mm width filled with 3.5 loops of WLS fibre. Number of loops was chosen by optimisation of the light collection and duration of the time response [5]. The ring groove has additional enter and exit grooves to lead out the WLS fibre ends. Fibre is glued inside the groove by BC-600 glue from BICRON [8] using a dedicated semi-automatic device that provides a winding of the fibres and uniform glue filling along the groove.

4.2 Fibre-to-fibre connection

Each single scintillator pad will be individually read out from both ends of the WLS fibre (Fig. 4). The ends of WLS fibre are long enough ($\sim 50\ cm$) to take the light from the cell out of the detector unit box. For the further transportation of light to the pixels of multi-anode phototube a long clear fibres will be coupled to WLS fibres by optical connectors shown in Fig. 6. The design of the connector is based on the development done for OPAL experiment [9]. The length of clear fibres varies from 0.7 to 3.5 m. All the fibres connected to the particular PMT have the same length

in accordance with front-end electronics specification [10],[11]. A clear fibre allows to transport the scintillator light from the SPD/PS planes over few meters to the MAPM without significant attenuation. Usage of the optical connector is defined by general assembly requirements.

4.3 Cell assembly

Before insertion into the groove the WLS fibres should be cut off with a needed length according to the diameter of the circular groove. After the fibre is glued into the scintillator and the pad is wrapped with 0.15 mm thick TYVEK or Teflon tape, that gives the minimal dead space between the adjacent pads and good reflection.

4.4 LED monitoring system

During data-taking, a LED control system will allow to synchronise read-out electronics and to monitor the time evolution of the PMT gain as well as the radiation damage and aging of the pads and fibres. We consider two possible solutions: one LED per cell, and one LED per 16 cells. The choice should be done in favour of cheapest and most reliable option which provides necessary stability and best functionality. To fix the LED to single cell it is packed into a small Plexiglas holder and glued at the pad centre (Fig. 8). At the same time the holder serves as a spacer holding the cell on the bottom of box after the box is closed. In case of one LED per 16 cells the light from LED is split into 16 optical fibres transporting it to each cell. The end of the fibre is glued into small prism against the mirror side. The reflected light enter the scintillator perpendicularly to the surface. The prism is glued to scintillator with an optical glue (Fig. 9).

5 Detector unit

The scintillator cells are grouped into the detector unit, that will be packed inside a square 476×476 mm^2 (SPD) and 478×478 mm^2 (PS) box yielding a total 26 boxes per one supermodule. Each unit module is self-supporting element. Because there are three regions with different cell sizes for the SPD/PS planes, the boxes will be filled with different number of pads with sizes divisible by 119 mm for SPD and 119.5 mm for PS planes. See Table 3.

5.1 Construction of box

The technology of box manufacturing was selected in order to provide a stiffness with a minimum amount of material between the adjacent cells in the neighbour boxes to reach minimal dead space of SPD/PS sensitive planes. The mechanical structure of the box is shown in Fig. 10. The monolithic box frame is manufactured using Carbon-Fibre Reinforced Plastic (CFRP) with the thickness of lateral wall 0.25 mm.

Table 3:

Region	Cell size of SPD (mm)	Cell size of PS (mm)	Detector unit
Inner	39.7	39.8	4 x 4
Middle	59.5	59.8	8 x 8
Outer	119.	119.5	12 x 12

This fabrication method was developed in INR RAN (by N.Golubev) and consists of one cycle polymerization process with defined curing parameters. Two prototypes of SPD/PS detector units were assembled with the boxes entirely made from CFRP and successfully tested during 1999 beam test [5].

The method allows to produce a wide number of complex shapes with high technical parameters. However the high cost of material have to assume compound construction of the box. Only lateral walls of the box will be made from CFRP, while the top and bottom covers are made from $\approx 2\ mm$ thickness Al plate or plastic. The assembly elements are made from plastic too and glued to lateral walls. The bottom cover is glued to the CFRP frame by epoxy and the top one is fixed by screws.

On the top cover there are output plastic ports disposed to allow an exit of fibres bundles out of the box (Fig. 11). They are made from plastic using a cheap pressure die casting technology. A LED power supply connectors are also fixed on the surface of the top cover.

5.2 Cell/fibres layout inside box

The design provides identical length for WLS fibres for all pads in the detector unit. All cells in detector unit are grouped in matrixes by $4 \times\ 4$ cells, and the fibres from each matrix are collected in one bundle ended by optical connector. The layout of fibres inside the box from one matrix is shown in Fig. 12. Bending diameter doesn't exceed 100 mm. To minimise the light losses during transportation of light from the cell to the optical connector, as an option, one can replace this part of fibre of $\sim 50\ cm$ length by clear fibre spliced to WLS one going out from scintillator in such case not far then by 10 cm. The choice on this option will be done after testing of prototypes in year 2000-2001.

5.3 Assembly of module

The module assembling proceeds as follows: the scintillator pads with glued WLS fibres after quality control tests are placed into the box. The ends of fibres are grouped by 32, inserted into a light tight flexible tube and gathered to an optical connector Fig. 13. The fibre ends will be inserted and glued into the optical connector, and after that cut and polished. Depending on number of scintillator cells inside the unit,

the boxes are equipped with one (in outer region), four (middle region) or nine (inner region) output ports and light connectors.

The unit modules are designed to be mounted on the supermodule support plate with screws prior to lifting them to the operation position.

6 Design and assembly of supermodule

6.1 Design of supermodule

The supermodules of the SPD/PS planes have identical design. Each supermodule consists of 26 detector units mounted on the long aluminium strip in two columns. PMTs are disposed on both top and bottom ends of the supermodule support outside the detector acceptance.

The detector units are connected to PMTs by optical cable consisting of bundle of 32 clear fibres closed in light-tight plastic tube. One end of the cable equipped with the optical connector (Fig. 6) to be coupled with connectors of the detector units disposed along the aluminium strip in accordance with the layout scheme shown in Fig. 14. Other ends of the optical cables are grouped by 4 and gathered to one PMT by means of photo-tube coupler shown in Fig. 7. Depending on the position of detector units inside the supermodule the length of clear cables varies from 0.7 to 3.5 m, providing the length of cables coming to the same PMT is equal. The trace scheme of optical cables is shown in Fig. 14.

The fibres are inserted into the corresponding holes of the optical coupler that holds the fibre ends in contact with the photo-cathode. After gluing in place the fibre ends are machined and polished. The holes are organised in precise matrix to fit the PMT' window in such a way, that they view by pairs the diagonal of corresponding pixel of the compact multi-anode photomultiplier R5900-M64, manufactured by Hamamatsu [12]. It has 12 stages and bialkali photo-cathode segmented in 64 pixels of 2×2 mm^2 each. Coupler holder and PMT-cookie assembly are disposed within the housing box (see Fig. 16) for mechanical protection, light-tightness, electrical and magnetic field shielding.

The design of PMT housing should be chosen in accordance with the electronic card dimensions, available space and required magnetic field protection. We will choose between three variants (Fig. 15,16,17).

The precise alignment of the coupler matrix relative to the pixels of MAPM is accomplished by using reference marks of PMT by a dedicated alignment tool, that is under development.

The top end of the supermodule aluminium strip is ridged out with an angle iron. Then it is hanged up to the carriage sliding along the base beam of the detector support. The bottom end with rather heavy steel plate is equipped with two binding beams of additional load for uniform stretching of aluminium strip.

6.2 Assembly of supermodule

The main idea is to perform the whole set of operations of assembly, cabling and control "on the table", leaving only the signal cables connection to be done after the supermodule is installed at the position of operation on the detector support. The assembly, transportation and installation of the supermodules can be done only with a special support cradle.

All stages of the assembly of the supermodule are shown in Fig. 18-20:

a) At the first stage the supermodule support is installed on a supporting table. At this position the top side is that where the clear cables with PMTs will be mounted.

b) After optical cables have been mounted according to the trace scheme shown in Fig. 14 and attached with a pitch of $\sim 0.5\ m$ to the support structure by plastic holders, boxes with PMTs will be installed and connected with optical cables.

c) Support cradle is attached from the top to the supermodule support. This is needed to prevent the support plane deflections during further manipulations.

d) The cradle with supermodule is lifted from the table and transported to the next assembly point.

e) For the detector units (boxes) installation the supermodule is maintained in the two layers stand. An access is granted from the both sides to install the modules from the top and to connect cables from the bottom.

f) All detector units are mounted in the place and connected with optical cables. The optical cables from boxes with connectors are pulled down through the holes in the aluminium strip. Each box is secured to the plate by four screws from the bottom side, being aligned with adjacent units.

Prior to installation to the working position all channels are tested with stand-alone DAQ system using LEDs and radioactive source.

g) After everything is assembled and tested, supermodule is ready for installation at the detector position.

h) Installation: supermodule is hanged up with bolts to the moving carriage of the detector support with a crane. The support cradle is detached and can be used for another supermodule assembly.

i) At the last stage, after the signal cables have been connected to the PMTs, the support cradle is removed and ready for the next supermodule assembly. After the supermodule have been installed, all channels will be checked by means of LED control system and radioactive source.

We assume that all stages of supermodules assembly are to be done in close proximity to the LHCb detector zone accessible by the crane. The necessary area is $12 \times 10\ m^2$. Time estimate for both lead and supermodules assembly is 4 months.

7 Assembly of detector

The assembly of the SPD/PS detector starts with the installation of the lead converter, that will be mounted on the base support beam by means of two structure channels (see Fig. 2). Lead converter wall is constructed from 8 independent strips that are 12 mm thick, 1 m wide and 7.9 m long, and covered with the stainless steel sheet of 0.5 mm thick from both sides. The stainless steel sheet will be glued to both sides of the lead under pressure. The manufacturing tolerance for the thickness of the lead sheets is typically 0.1 mm. The strips were chosen because of its convenience for the manufacturing and assembly by the crane facilities inside the experimental hall. The top ends of lead strips are ridged with the two channel beams and from the bottom with the zee-beams with additional load.

Before transportation to the operational zone the lead strip is secured on the support cradle. Then it is lifted by the crane and transported to the place of installation, where the I-beam on the top of the lead strip is fixed to the base support beam by bolts. On the base support beam there is a set of tuning bolts, that are connected with the main beam to correct arising deformation. To avoid the swing-effect the bottom ends of strips are inserted between two channel beams disposed at the bottom of the support frame. After the channel beams have been bolted to the I-beam, the support cradle is dismounted from the lead strip and may be used for installation of the next one. After the installation all lead strips are joined together with a flat hinges. The rails are mounted on the structure channels on the top of the lead strips.

The procedure of the SPD/PS detector assembly is very similar to the mentioned above for the lead converter. Before the installation, a support cradle will be temporally attached to the supermodule support in order to allow the supermodules to be moved to the operation position. The supermodules are mounted on the separate moving carriages that are installed on rails disposed along the base beam and can be moved in horizontal direction. After the assembly of the detector parts is done, they can be rolled to its final position.

The signal cables routing is made flexible allowing the movement of the detector without cable disconnection.

When the SPD/PS detector is installed to the working position the place around is rather limited so that only the perimeter of the support frame can be reached during a short access period. Therefore during repairing or maintenance interventions the halves of the detectors will be moved out of working position along the main support beam.

8 Monitoring

Stability control and monitoring are mandatory for the SPD/PS detector performance. Parameters of the detector operation can be determined with different subsystems that are discussed below. But one of the most important application of the monitoring system is to provide precise timing reference to be used for inter-channel synchronisation.

8.1 LED calibration

Light injection system should provide a short-term relative calibration of the detector channels and monitor their parameters over the lifetime of the detector. It should be reliable, easy to use and not too much expensive. Among well known systems based on laser, UV lamp and LEDs the latter looks much more preferable [13] due to their modularity, lack of moving parts and high performance. A number of such systems [14, 15, 16, 4] reveal a long-term stability of 1 % and good uniformity in the light distribution over a few thousands of channels.

In case of the SPD/PS detector the possible calibration system may be based on the prototype designed for ALICE PHOS detector [17]. The control unit is located in the rack on the top of the detector and the LED driver PCB is positioned near the detector unit. They are connected by a flat cable, thus minimising the number of cables to the movable detector wall. The prototype was designed for using with slow electronics and cannot be applied as it is for our needs. Modification of the output chains of the driver should be made.

Another solution can be the using of one LED to illuminate a number of cells. In this case the LED and the light mixer are installed on the support structure outside the detector unit. Clear fibres from the light mixer go into the detector unit box where the second light mixer redistributes the light to the particular cells. The number of cells for half of the SPD/PS wall is 2976. The driver has 64 outputs, i.e. the mean number of channels fired by one LED is less than 50, far below 800 [18] or 250 [16].

To provide relative synchronisation of channels fast LED response is needed to reproduce the particle signal in the fast electronic chain. The fast and bright LED generally is more expensive. This can effect on the trade between two options. The requirements to the time response of the LED is another subject of Monte-Carlo study.

8.2 Photomultipliers gain monitoring

It is well known that photomultiplier gain is a subject of long- and short-time variations for many reasons, such as temperature and vacuum changes, thermal and chemical reactions in the material etc. Monitoring of the stability of PMTs is essential for understanding of the detector response.

To control the PMT gain it is necessary to send a known amount of light and read

the answer. Current mapping of the optical cables from PS and SPD to MAPMT do not leave free channels. Fortunately we do not need to light up PM pads individually. A few clear fibres before they come to PMT, passed through a light diffusion box with LED and have been illuminated by green light. They will pick up enough light for calibration. The boxes (one per PMT) should be situated near the PM assembly to exclude optical cables influence.

Illuminating of fibres can be performed by equipping every diffusion box with its own light pulser or by distributing light pulses from one common light source through clear optical fibres. In the latter case monitoring of light source itself can be done in a simple way with a PIN photo-diode.

The width of LED signal spectrum defined by the photostatistics provides absolute scale for the detector response and can be used for the control of linearity of the readout chains.

8.3 MIPs calibration

The SPD/PS detector have a possibility to be calibrated during the run using MIPs from the flux of produced particles. Trigger information on the type of particle (hadron, muon) as well as cuts on energy deposited in ECAL and HCAL can provide a reasonable way for on-line monitoring of every channel. A precision of better than 5 % was achieved with this method for in-situ calibration of ZEUS presampler [19]. Monte-Carlo study should be done to evaluate the overall accuracy of this method in case of the LHCb environment.

This method of calibration depends on the accuracy of the preliminary calibration and will converge quickly only if it was precise enough. Unlike LED calibration this one needs some run time to accumulate sufficient statistics.

8.4 Calibration with radioactive source

The movable radioactive source provides a natural tool to inter-calibrate cells, monitor the combined response of cell, fibre, connectors and PMT and ensure quality control of individual channels. It enables also to compare the cell response with those measured during production stage with the same kind of source.

The source scan is a time consuming procedure. We will have the possibility to make it only a few times per year during the shutdown periods. Partial scan could be done in case of troubleshooting or replacement of the detector units. This is one reason why we do not intend to install this system permanently. Another one is a very stringent condition in Z direction for PS and SPD that does not enable to do it.

Instead, this system could be installed only when it is necessary and when the detectors are taken out of the working position. This has the advantage of scanning at the same time both detectors (PS and SPD) due to the small distance in between.

There are different options under study of calibration with a radioactive source. The simplest one is the current mode operation with a signal taken from the last

dynode of the PMT that is common for all PMT channels. In this case there is no need in synchronization and using of the standard electronics, only a stand-alone DAQ system is nesessary. More complicated options are discussed but they require to add some additional features to the front-end electronics.

9 Quality control

Two issues are the main goal of quality control. First is to keep the performance of all tiles at top quality. Second, to minimise the production cost. The latter means that quality control must be at every step of fabrication process, starting from analysis of raw materials and up to the final certification of each scintillator cell before assembling.

There is a good experience gained by different experiments [20, 21, 22] in mass production of scintillators. Our aim is to apply worked out reliable and effective quality control methods while taking into account specific features of our detector. The experience gives also some useful values of the constrained cuts for parameters under control reached in the particular experiment. In the following we list the stages and appropriate procedures we intend to use to monitor cells production.

9.1 Raw materials

Total amount of plastic scintillator necessary for PS and SPD walls is $\approx 1.5\ m^3$. It will be delivered from one manufacturer but in a few ingots. Production will be spread over two years period and we will have to be sure that the properties of bulk scintillator are constant and of the good quality. To monitor the light output from different ingots small samples of scintillator of fixed dimensions $\approx 1cm^3$ are cut out, polished and tested with the radioactive source in the stand.

Two another important parameters, transparency to the scintillator' own emission and purity of raw materials used are measured using chemical analysis technique for a few cells or specimens from the same ingot. Some details specific to scintillator cell production could be found in [22].

9.2 Cell production

After mechanical processing and polishing of cells two checks should be performed. First is dimensional one and the tolerance of $\pm 0.1\ mm$ (3σ) for 6 mm scintillator plates was achieved for CDF megatile production [20]. Another one is a visual inspection to exclude samples with cracks and scratches and to evaluate surface quality. After this stage every tile receive its own number that must be engraved on it.

All fibres should pass an optical test to reject those that could be damaged during transportation or unpacking. If splicing is used, the test must be repeated. This is important to keep under control the output of the welding machine.

Optical tests should be fast, reliable and easy to handle. We suppose to use LED in conjunction with PIN diode to measure the transparency of fibres. The similar devices called "optical power meters" (OPM) are routinely used to check out optical cables and connectors for optical networks. They are portable and can be used in situ. Typical accuracy of OPM in relative mode is 3%that is quite enough to make a $\pm 10\%$ cut [20] to reject bad fibres.

Gluing fibres into the groove is another process, that may suffer from large variation in quality. This is mainly because it can be hardly made fully automatic. It may contribute to the total variation of relative light output even more than that of fibres [20]. Fast optical test of light trapping by WLS fibre could be thus useful before scintillator wrapping. This can be easily done with OPM by injecting blue light into the scintillator cell from a number of fixed points in a sequence and reading light output with the fibre.

9.3 Connectors

Fibres from 16 tiles (4x4 cell) are grouped and feed to the same optical connector. The quality of multi-pin connectors is of great importance due to the possibility of the occasional large light losses. Above the construction of the connector itself the optical contacts play crucial role for the level of light losses. We have designed a cutting and polishing device based on the construction described in [23]. It is in the production stage now and will be tested soon. For the quality control of the optical connector the visual inspection of its surface under reflection angle with a microscope should be done. This procedure is especially useful at the initial stage of cell production for maintenance of the technology process and can be done on a random basis at the rest of time. Another way is to use OPM to check out every fibre in a bundle in semi-automatic mode.

9.4 Certification of cells

Cells that passed all tests are wrapped using white reflective paper (TYVEK) and assembled in a detector unit. It will be scanned with radioactive source in the stand to measure the absolute light yield and light yield homogeneity. The level of cross talks should be measured as well to check for possible light leakage between tiles. Some number of detector units should be tested in the beam of minimum ionising particles to get direct comparison with in lab test data.

9.5 Data management

All data collected during production stage will be stored in the local data base in a non-destructive way. These include dates of production of raw materials and scintillator ingots and their numbers, results of tests, etc. for every cell together with its number and time stamp for every operation. Knowledge of individual parameters of

all produced cells will allow to trace their time evolution under the effect of physical processes like aging or accumulated dose. These data will be used also in areas such as detector slow control, calibration and maintenance.

Acknowledgements

We gratefully acknowledge the permanent support and fruitful discussions from J. Lefrancois. We are kindly indebted to A. Schopper and P. Perret for reading the draft version of this note and sending us their comments. The help provided by our colleagues from LHCb calorimetry group is especially appreciated.

References

[1] LHCb Collaboration, LHCb Technical Proposal, CERN/LHCC 98-4 (1998).

[2] V.I. Kryshkin,A.I.Ronzhin, NIM A247 (1986) 583 CDF II Detector TDR, FERMILAB-Pub-96/390-E, 1996

[3] M.M. Aggarwal *et al.*, VECC-NEX-98002, NIM A424 (1999)395

[4] MINOS Collaboration, Technical Design Report

[5] S. Filippov *et al.*, Experimental performance of PS/SPD prototype, LHCb 2000-031, CALO

[6] KURARAY Corp., 3-10, Nihonbashi, 2 chome, Chuo-ku, Tokyo, Japan

[7] K. Hara *et al.*, NIM A411(1998) 31

[8] BICRON Corp., 12345 Kinsman Rd., Newbury, OH 440, USA

[9] G. Aguillion *et al.*, NIM A417 (1998) 266

[10] S. Bota *et al.*, Scintillator Pad Detector Front-End El ectronics, LHCb 2000-027, CALO

[11] G. Bohner *et al.*, Very Front-End Electronics for LHCb Prteshower Detector, LHCb 2000-047, CALO

[12] HAMAMATSU Photonics KK, Electron Tube Center,314-5,Shimokanzo, Toyooka-village, Iwata-gun, Shizuoka-ken, 438-1 Japan.

[13] P. Harris *et al.*, NuMI-L-550, 1999

[14] T. Peitzmann *et al.*, NIM A376 (1996) 368

[15] D. Autiero *et al.*, NIM A372 (1996) 556

[16] M.H.R. Khan *et al.*, NIM A413 (1998) 201

[17] ALICE Photon Spectrometer PHOS TDR, p.94, 1999

[18] B. Anderson *et al.*, hep-ex/9810040

[19] A. Bamberger *et al*, NIM A382 (1996) 419

[20] P. de Barbaro *et al*, UR-1371, 1994

[21] M. Lebeau *et al.*, CMS TN 95/024

[22] S. Barsuk *et al.*, Facility to control the production of shashlik type electromagnetic calorimeter, LHCb CALO-044, 2000

[23] F. Adamian *et al.*, ATLAS Internal Note TILECAL-NO-126, 1997

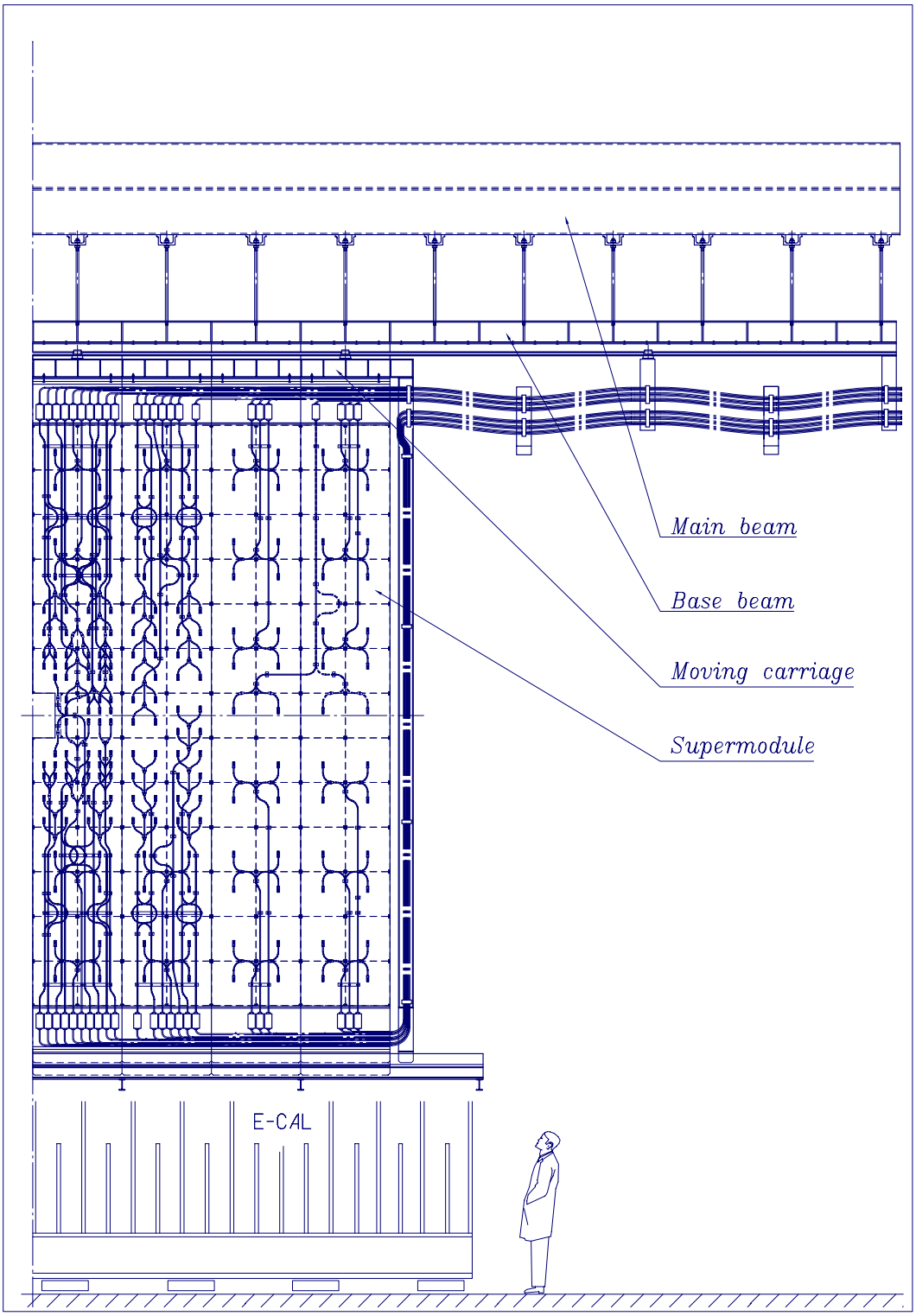

Figure 1: The layout of one half of SPD/PS detector. Optical and signal cables routing is shown.

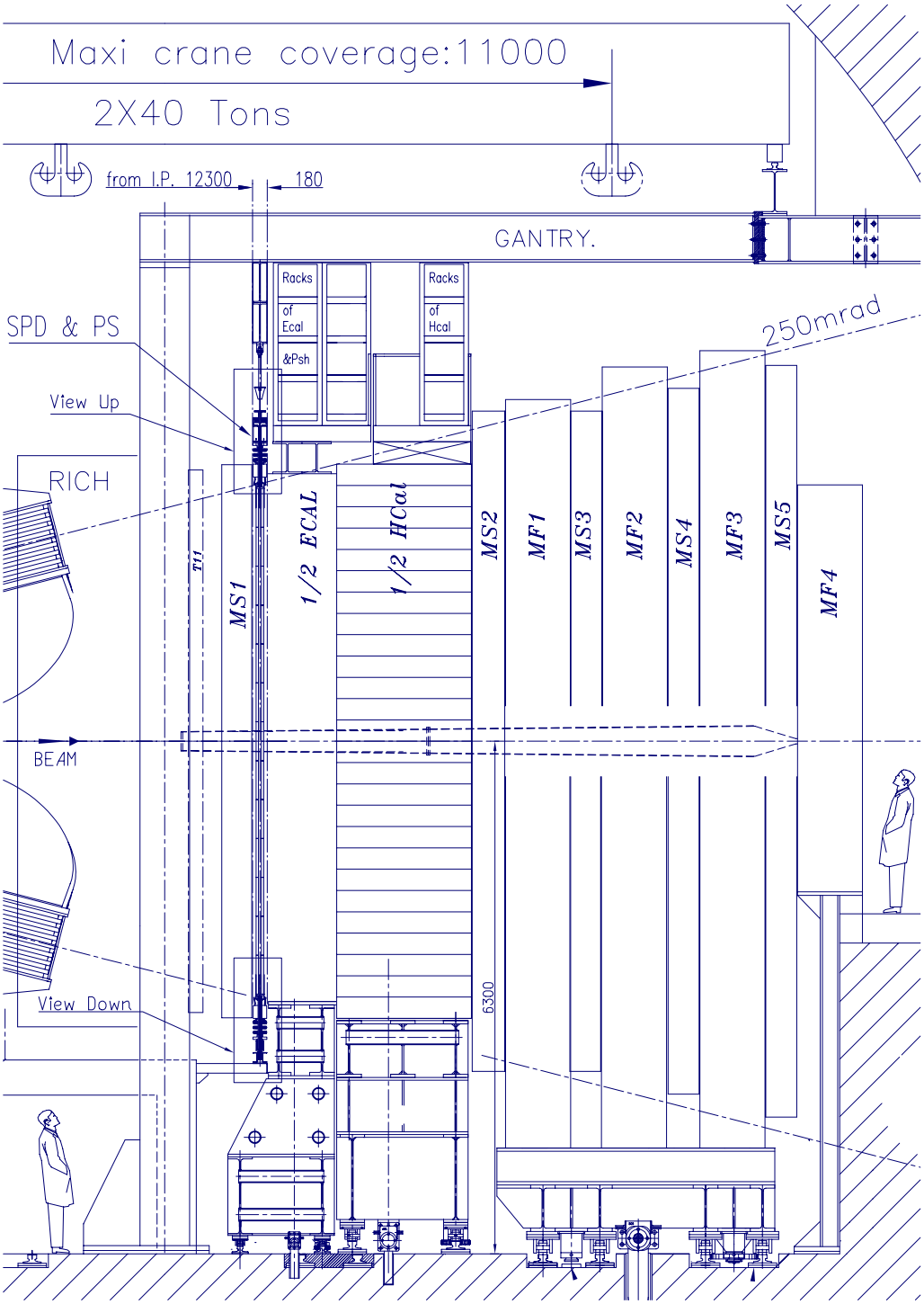

Figure 2: The side view of SPD/PS detector.

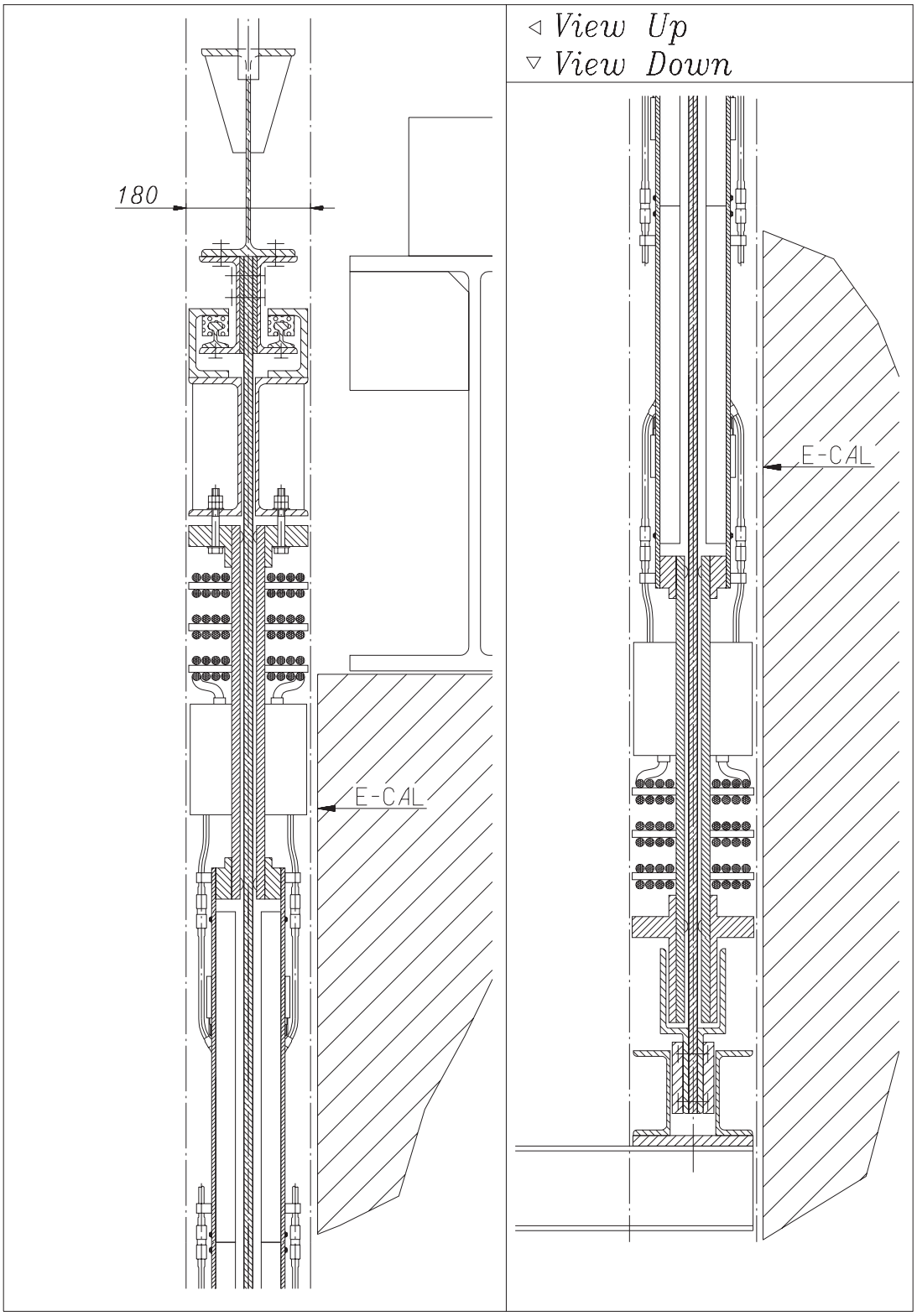

Figure 3: Upper and lower parts of SPD/PS detector along the beam axis.

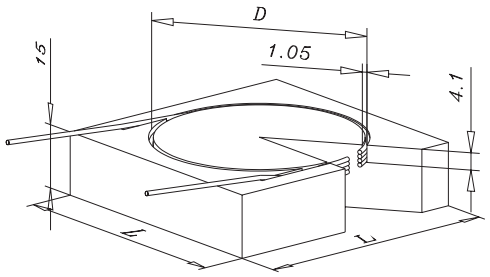

Region	L,mm (SPD)	L,mm (PS)	D,mm
inner	39.2	39.5	37
middle	59.0	59.4	56
outer	118.4	119.1	110

Figure 4: Scintillator cell design.

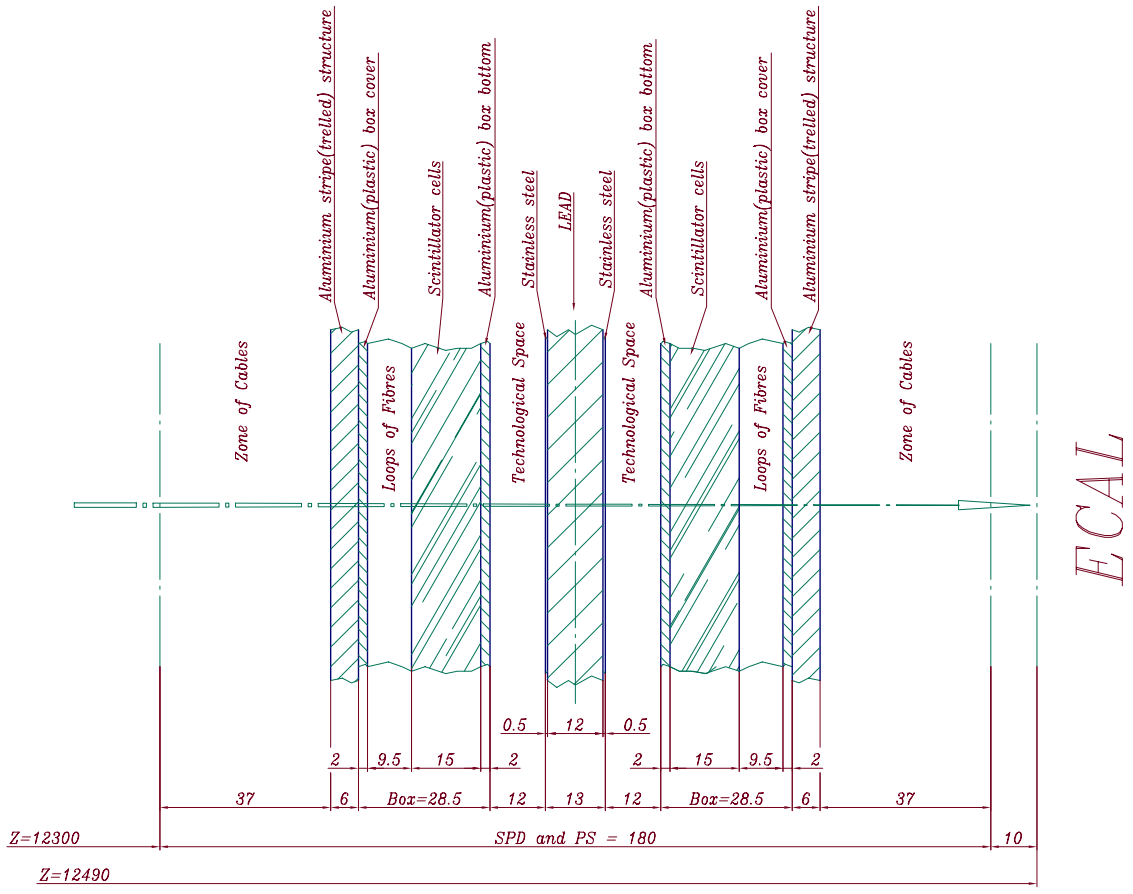

Figure 5: The material budget of SPD/PS detector along the beam axis.

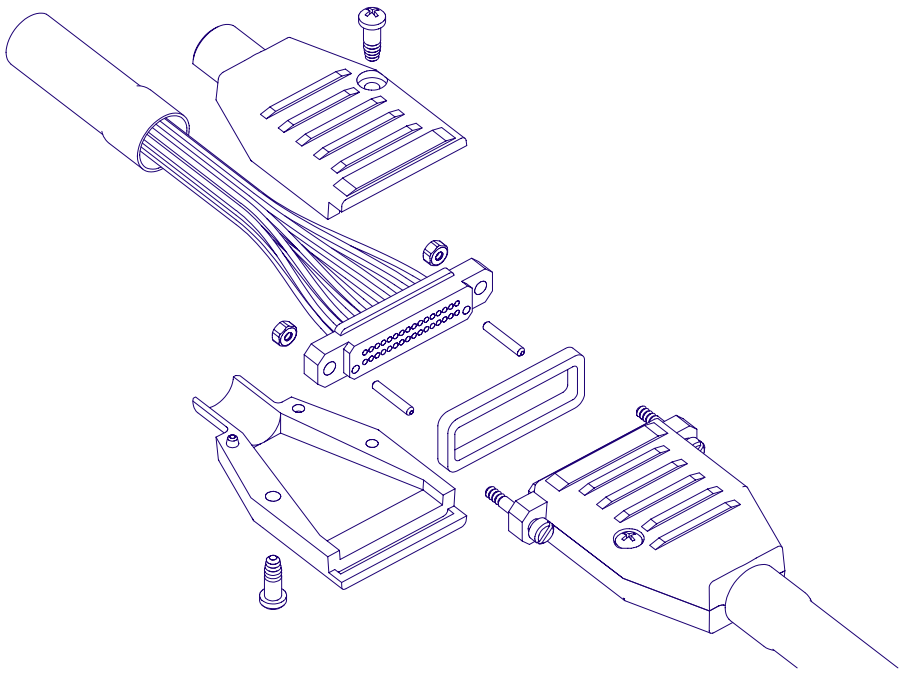

Figure 6: View of fibre-to-fibre optical connector for 32 fibres. The precision of the fibres connection is achieved with two Dowel pins. Fibres are glued in holes machined with high accuracy in Delrin plastic.

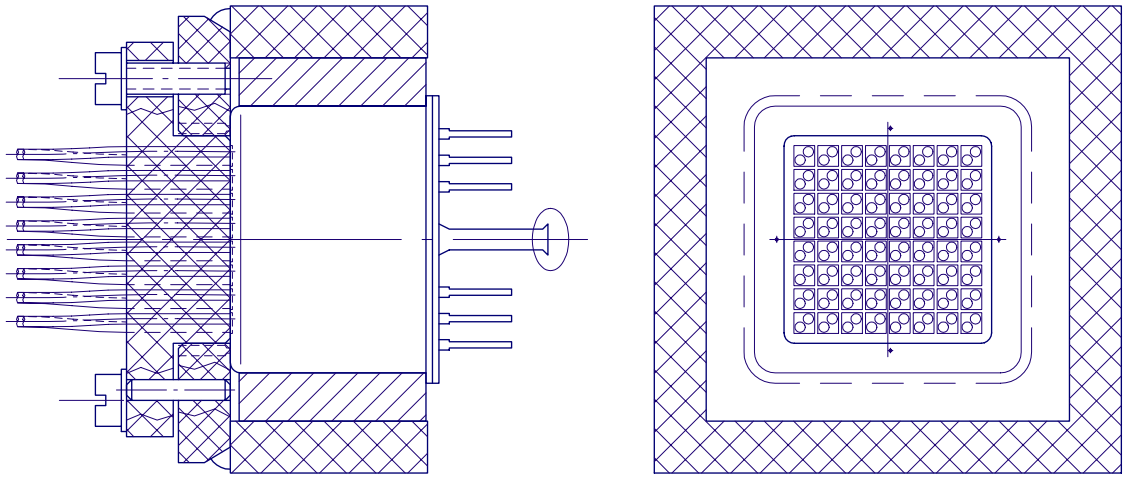

Figure 7: View of fibres-to-PMT optical coupler.

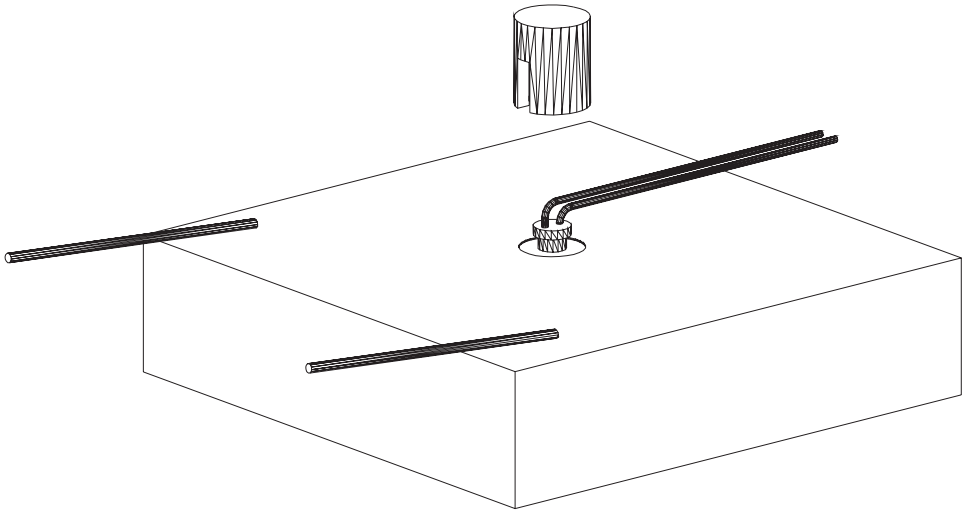

Figure 8: LED glued on scintillator pad.

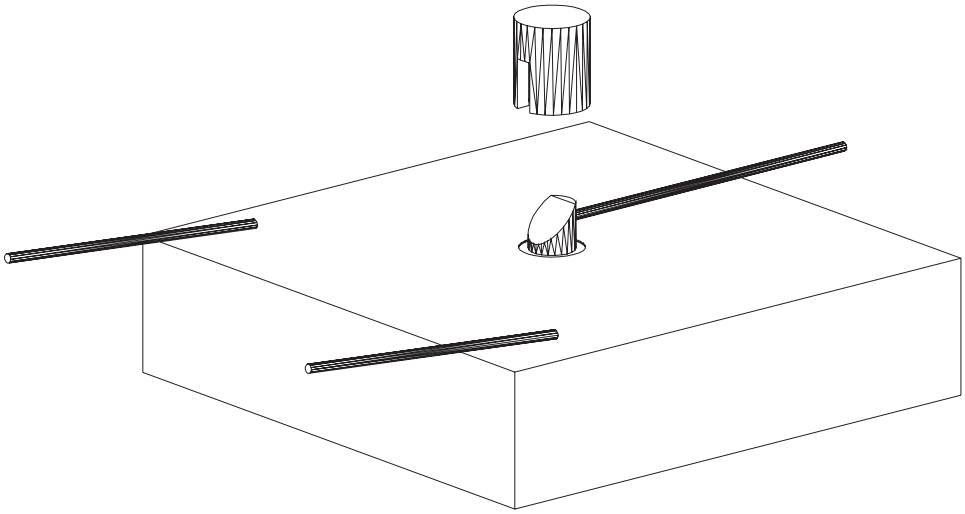

Figure 9: Monitoring fibre coming to scintillator pad.

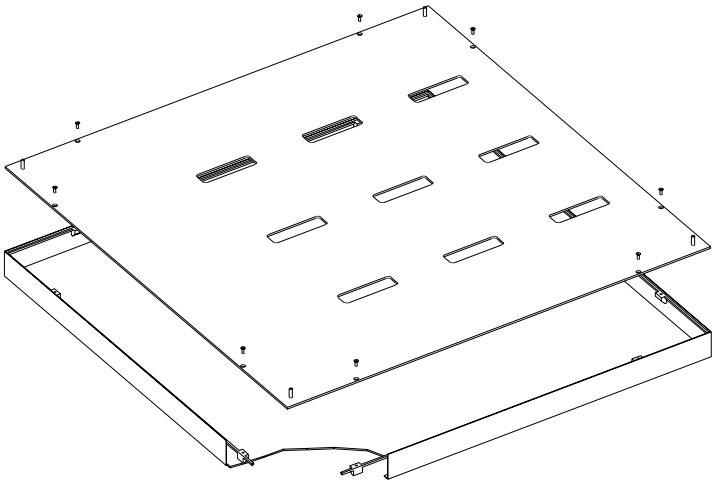

Figure 10: Design of module box.

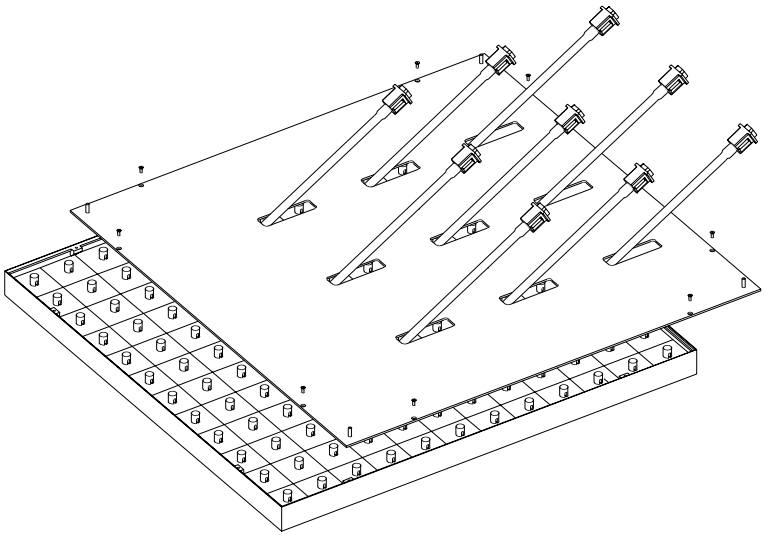

Figure 11: Design of module box. Assembly elements.

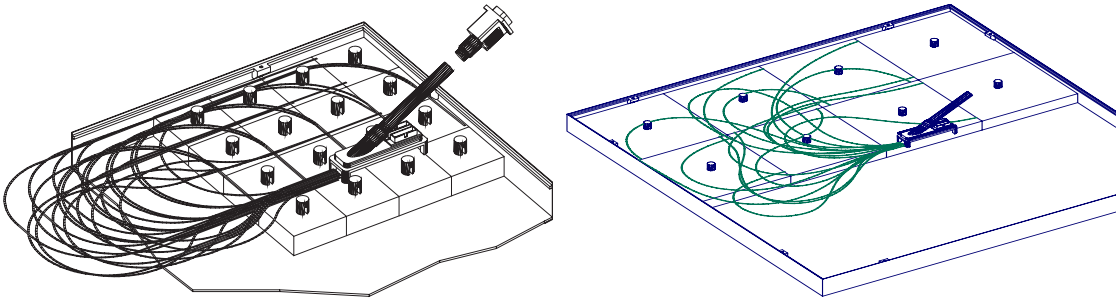

Figure 12: Fibres routing inside the inner (left) and the outer (right) module box with pads.

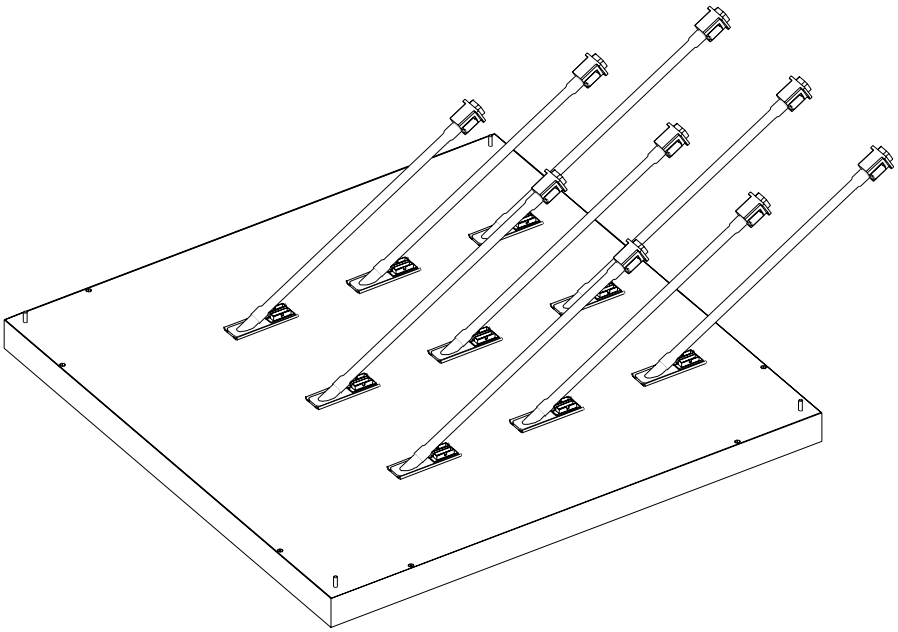

Figure 13: View of assembled module with connectors.

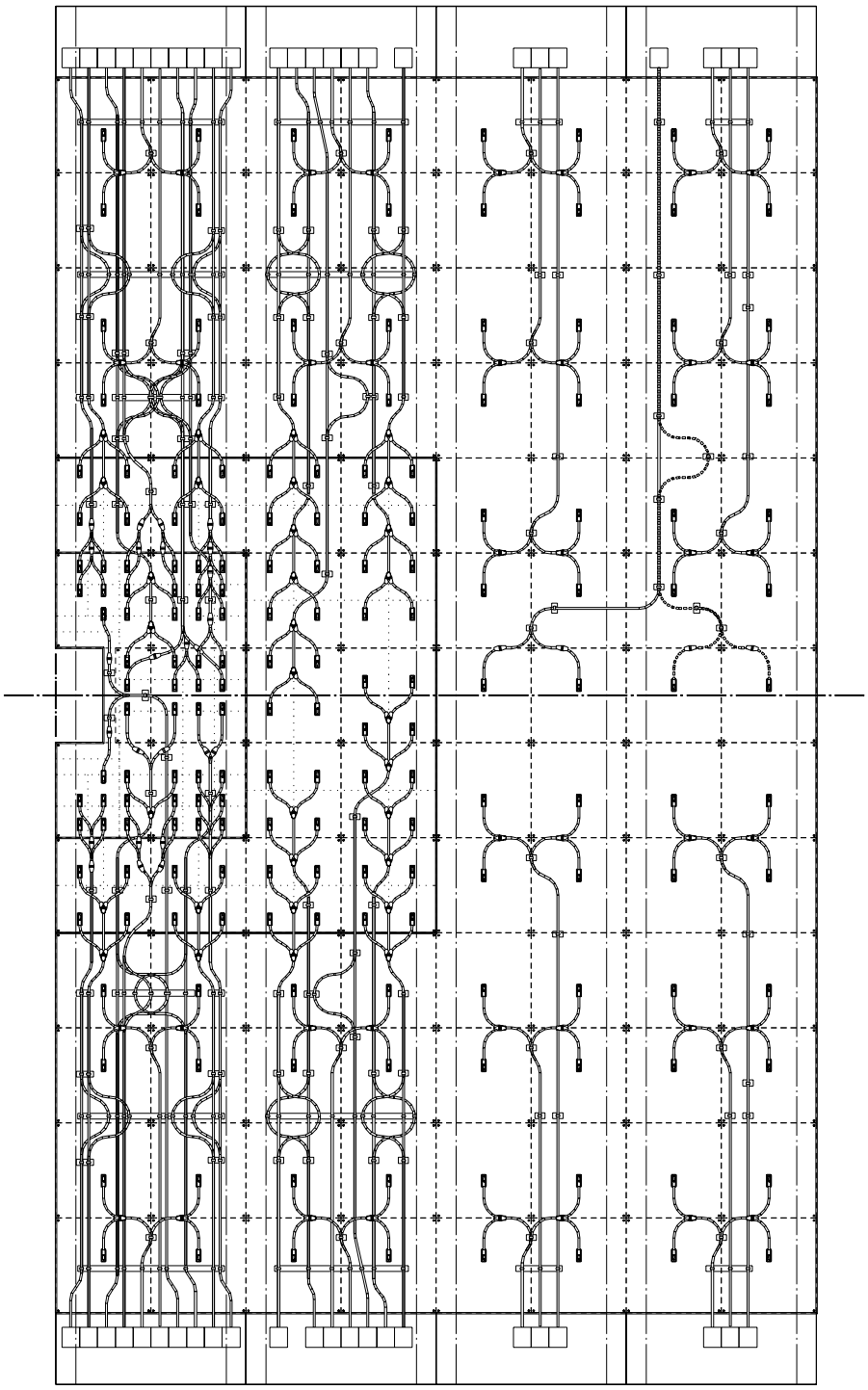

Figure 14: Optical cables routing.

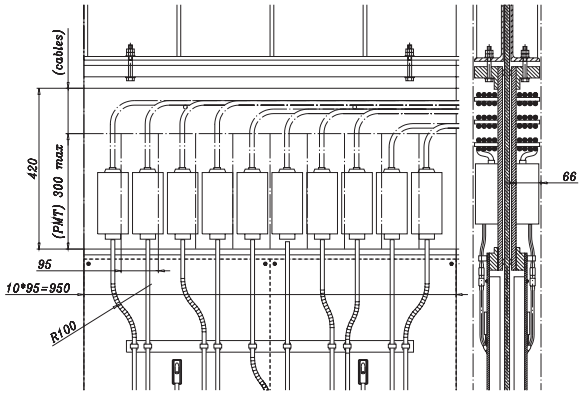

Figure 15: PMTs layout, variant 1.

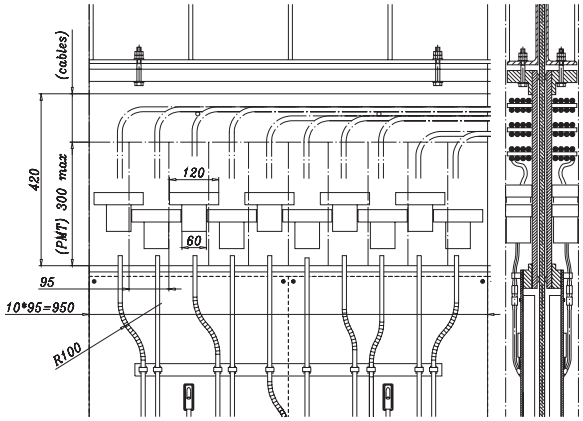

Figure 16: PMTs layout, variant 2.

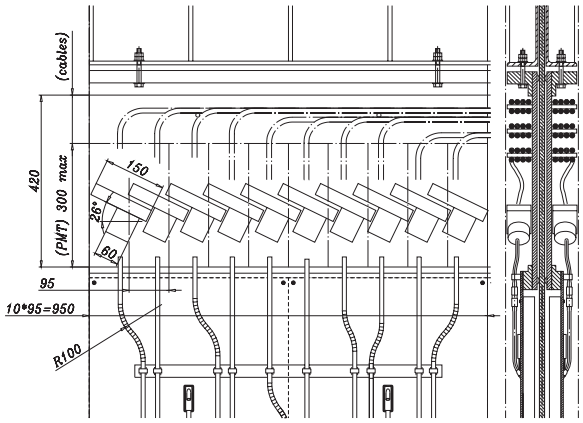

Figure 17: PMTs layout, variant 3.

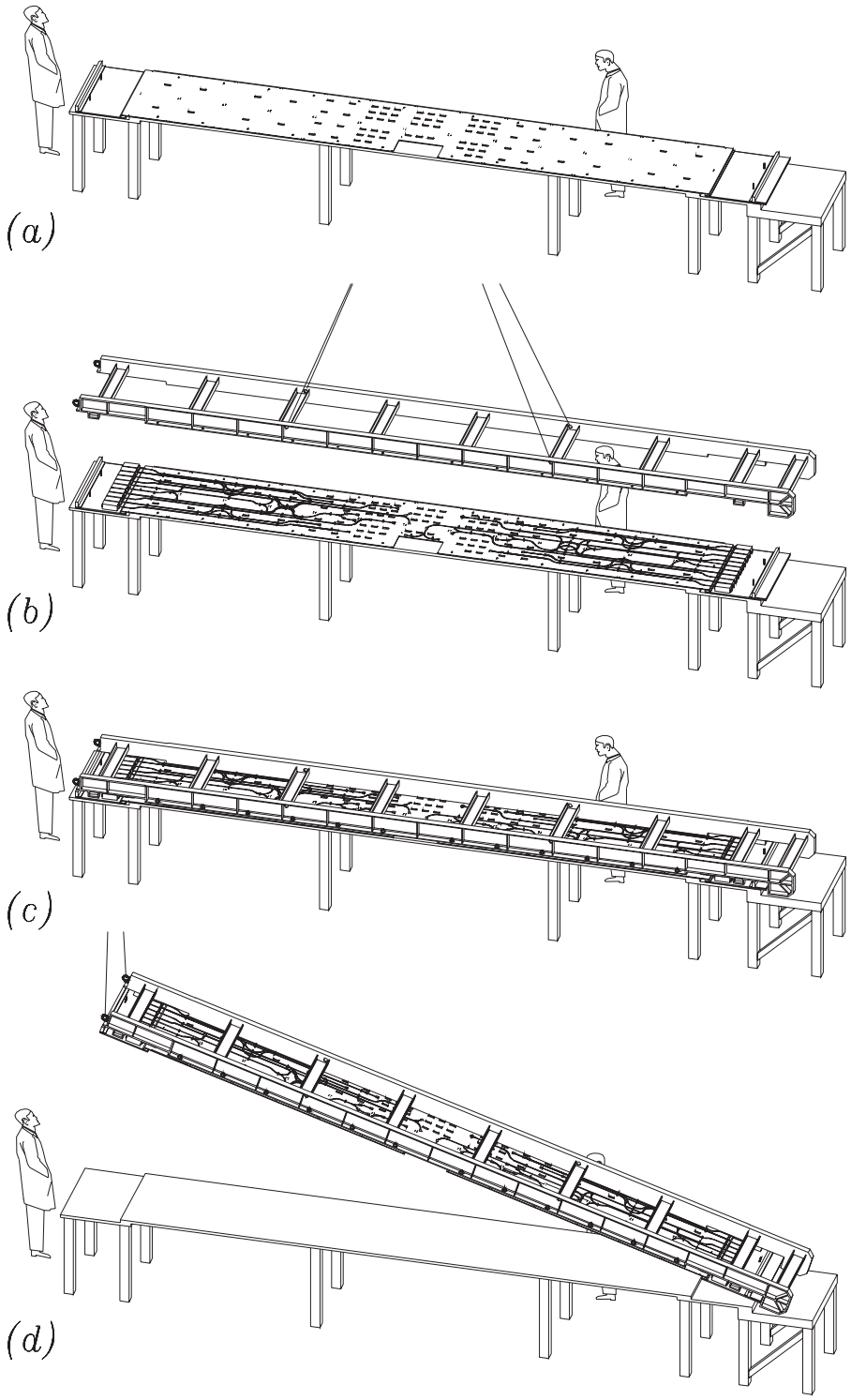

Figure 18: Assembly of supermodule - 1.

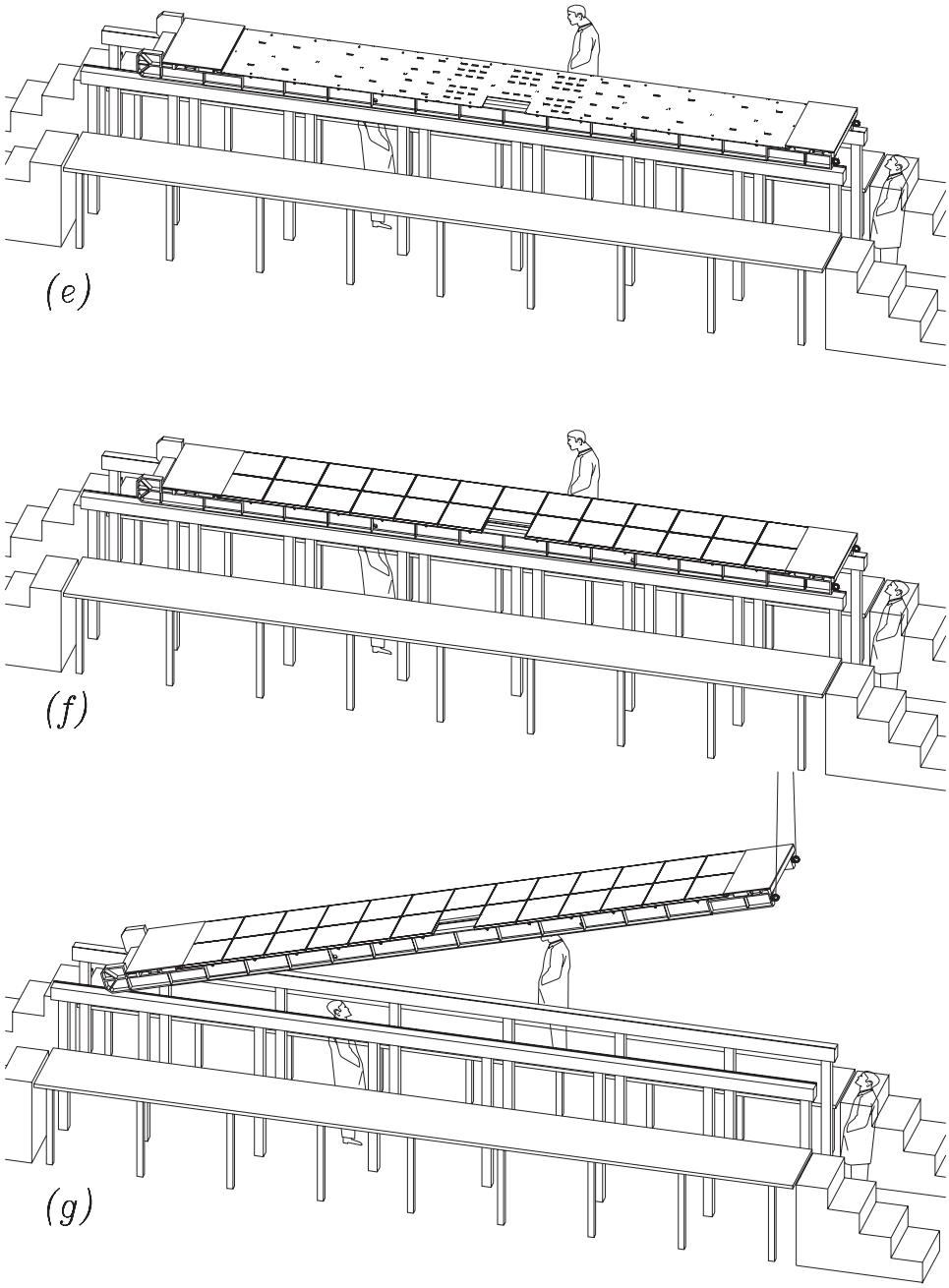

Figure 19: Assembly of supermodule - 2.

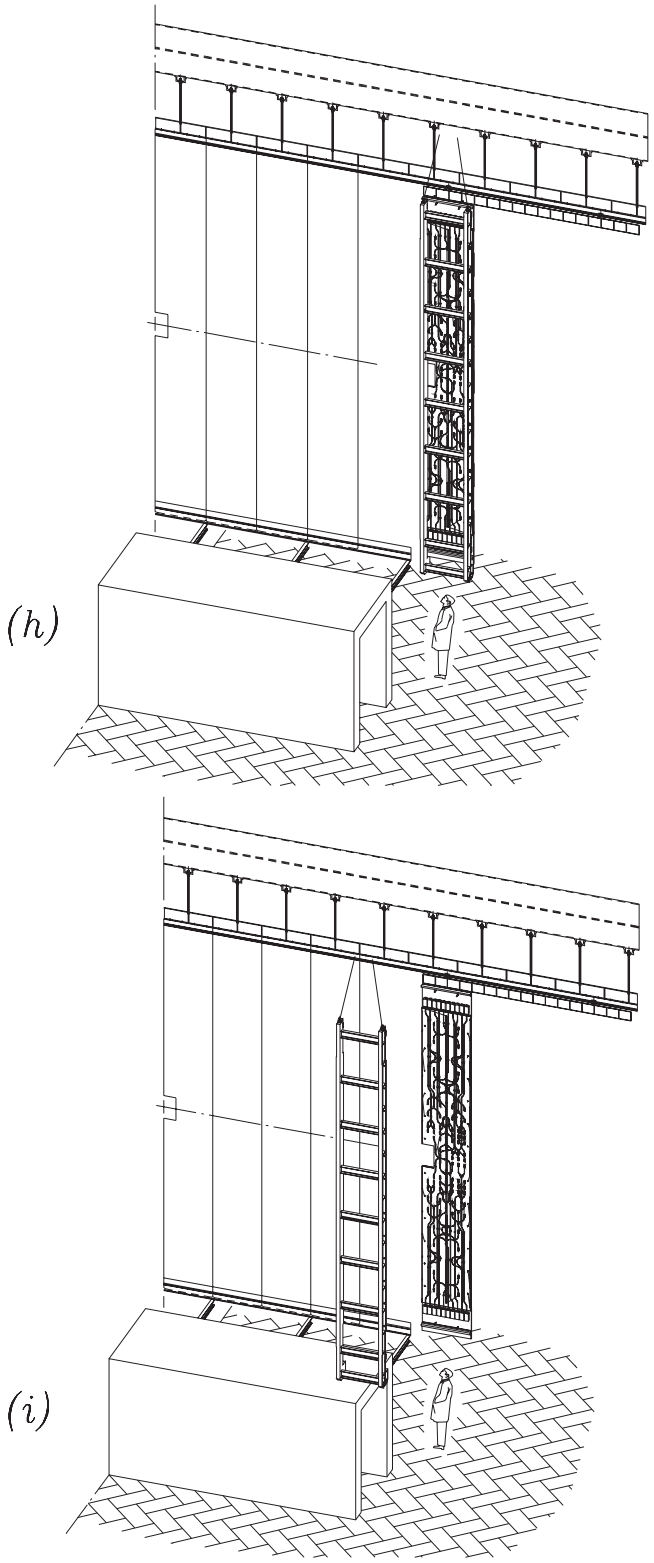

Figure 20: Assembly of detector.